Simulating the Impact of Deciduous Trees on Energy, Daylight, and Visual Comfort: Impact Analysis and a Practical Framework for Implementation

Jessie Pan[1], J. Alstan Jakubiec[2]
[1]University of Toronto, Toronto, Canada
[2] University of Toronto, Toronto, Canada

Abstract

The impact of dynamic landscape elements on daylight and energy is not typically considered in building performance simulations. This paper describes a new method of creating detailed, seasonally varying tree models that integrate gap fraction, seasonal leaf drop, regrowth, and colour change schedules, as well as dimensions and heights of tree canopies. Twelve urban deciduous tree species in Vancouver, Canada were measured to create detailed deciduous tree models. These models are applied within annual daylight and energy simulations and are compared to simulations with no tree, an evergreen tree, an evergreen tree with no canopy gaps (solid), and a detailed tree with no colour change.

Introduction

Trees produce environmental, economic, social, and psychological benefits in human habitats and recreational areas (Coder, 2017). Heat island mitigation, shade, air cooling, and decreasing wind speed (Akbari et al., 2001) benefit urban settings. Building performance benefits include glare reduction, shade use reduction, and lower energy consumption. Studies from Donovan & Butry (2009), Hwang et al. (2016), G. E. McPherson et al. (1994), Simpson & McPherson (1998, 2003), and Simpson (2002) all found that urban landscape trees can dramatically reduce energy demand in buildings. By integrating thermal and visual comfort with energy-efficient design strategies, the energy consumption of buildings can significantly decrease, thus acting as a sustainable design strategy (Compagnon, 2004; Nasrollahi & Shokri, 2016). Trees should be integrated in architectural and urban site planning through simulation tools so designers can assess and maximize daylight availability, reduce glare problems, and contribute to passive heat gains and cooling load reduction (Compagnon, 2004).

When predicting the influence of trees on daylighting, visual comfort and energy performance, simulations often use solid or simplified trees that are modelled as opaque geometries or with a uniform transmittance coefficient (Balakrishnan & Jakubiec, 2016; Wilkinson, 1995). The IES Daylight Metrics Committee recommends that trees should be modelled as opaque solids with a reflectance of 20% (IES LM-83, 2012). This is seen in the work of Szkordilisz & Kiss (2016), Tregenza & Wilson (2011), and Simpson (2002). Other lighting simulation standards do not provide guidance on modelling trees.

Trees are formally complex, resulting in fluctuating light transmittance phenomena—reflection, diffusion, obstruction, and attenuation—that vary with solar position and weather (Balakrishnan & Jakubiec, 2016; Villalba et al., 2014). For example, light transmission through tree canopies is dependent on the solar incident angle along with canopy size, leaf area densities, and direct gap fractions along the solar vector. It is important to accurately account for light passing through a canopy by the time of year and the position of trees relative to a building surface. Deciduous trees are particularly sophisticated due to tree phenology and leaf senescence that impact their foliage density and colour throughout the year. Diverse genera and species are difficult to model as they exhibit an array of characteristics such as seasonal and morphological differences. These complex and variable temporal effects of trees are often estimated or entirely ignored due to these complexities; however, these effects have been modelled by Simpson and McPherson (2003). In a thermal model, they applied an assumed leafless shade fraction of 30% from December to March and a foliated shade fraction of 85% from April to November.

Methodology

The twelve most common deciduous street trees in Vancouver, Canada were studied through literature review and direct physical measurements to create detailed tree models for simulations. Data on tree colour, canopy size, height, and scheduling for leaf drop, regrowth, and colour change have been collected from literature, (see Figure 2) where the gap fractions of trees were calculated from measurements, based on the image processing methodology described by Balakrishnan and Jakubiec (2020). Daylight and energy simulations of a typical office space were then run using a Radiance-based lighting simulation workflow with dynamic deciduous tree models. Finally, we compared these most-detailed deciduous tree workflows with simplified simulation workflows: no colour change,

evergreen trees, evergreen trees with no canopy gaps, and no trees.

Tree Selection

The twelve most common deciduous street trees in Vancouver, Canada, were selected from the City of Vancouver Open Data Portal's Street Trees dataset: *Acer platanoides, Aesculus hippocastanum, Betula pendula, Carpinus betulus, Fagus sylvatica, Fraxinus americana, Magnolia kobus, Malus floribunda, Prunus cerasifera, Prunus serrulata, Quercus palustris, and Tilia x euchlora.* The *Acer platanoides*, commonly known as the Norway Maple, is a non-native invasive species, however, it is often cultivated and planted as a street tree due to its decorative properties. The street trees dataset was used to map physical locations of tree species and identify them for photography, direct measurement, and leaf sample collection.

Tree Measurements

For each species identified, five to seven individual trees were measured based on requirements for their measurement–a background of an open sky with little to no surrounding obstructions. Measurements were collected between June 1st and July 20th, 2021, on clear, sunny days with no cloud cover and the sun high in the sky. In sum, 154 measurements were collected using regular photography at vertical and lower angles to avoid background context seen through the tree canopies (see Figure 1) (Balakrishnan and Jakubiec 2020). For each measurement, well-exposed images of tree canopies against a neutral background (diffuse sky) were automatically extracted from the background, thresholded into solid and void (Nobis & Hunziker, 2005), and processed to assess the total gaps through the canopy from a specific position and view direction. This process is repeated at multiple tripod locations to collect multiple, varied angular measurements per tree; however, for some trees only a few measurements could be taken due to their immediate urban context. This data along with canopy dimensions and tree height was used to create three-dimensional tree models (see Figure 2).

Each image was run through Balakrishnan and Jakubiec's floodfill algorithm to calculate the gap percentage of the tree canopy—the percentage of direct sky visible through the canopy bounds, illustrated in part by Figure 1.

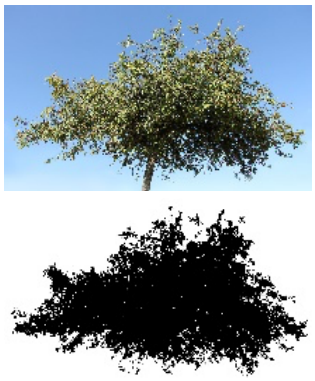

Figure 1: Base photograph (M. floribunda) and threshold result showing canopy gaps.

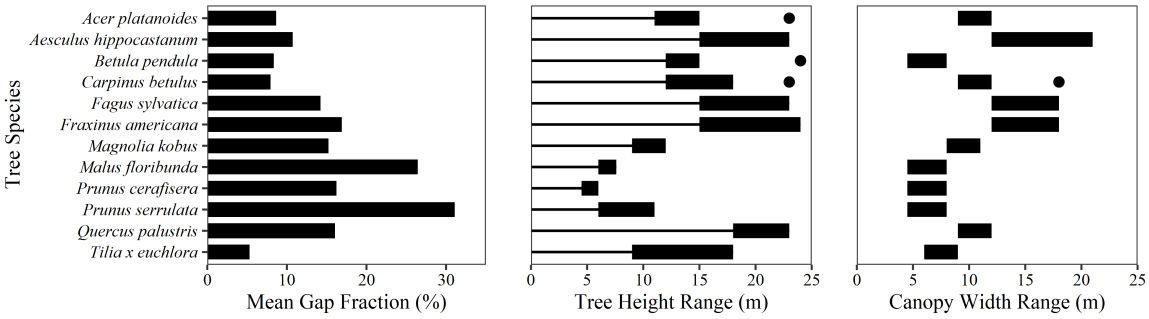

Figure 2: Measured gap fractions from image processing and collected data on tree height range and typical canopy diameter.

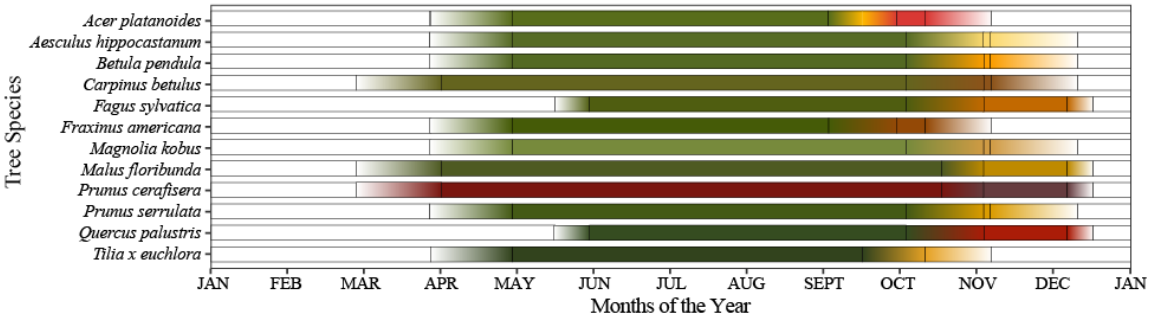

Figure 3: Temporal schedules of leaf growth, leaf colour change, and leaf drop. Actual measured colours are used for each tree species except for the A. hippocastanum autumn colour.

Timing of Seasonal Colour Changes, Leaf Drop, and Regrowth

The timing of tree colour change, leaf drop, and leaf regrowth necessary to produce temporal schedules for building performance simulation are not commonly found within forestry databases. Phenological properties of trees may differ due to climate, changes in temperature (Fu et al., 2018), soil quality (Pausas, 1997), and location (Schaber & Badeck, 2005). We collected temporal tree information from Ticknor's study of landscape tree performance (1973) for twelve deciduous species. Portions of the phenology information for *Aesculus hippocastanum*, *Magnolia kobus*, *Malus floribunda*, and *Tilia x euchlora* were collected from other literature (De Jaegere, 2016; Moesker, 2019; *Observational Data USA National Phenology Network*, 2021; *Observations*, 2021). If the specific species had no phenology data, the closest species in the same genus was used (*Aesculus carnea brioti* (leaf drop), *Fraxinus ornus* (colour change and leaf drop), *Tilia cordata* (colour change), *Tilia americana* (leaf drop)). Data on typical canopy size and height (see Figure 2) for all twelve species were collected from the Landscape Plants Database at the College of Agricultural Sciences - Department of Horticulture at Oregon State University (Breen, 2021) and the Environmental Horticulture Database from the University of Florida (Gilman & Watson, 1993).

Leaf reflective colour properties were measured using a Konica Minolta CM-2500d spectrophotometer (Jakubiec, 2016) using a three average sample per leaf and tree. Where possible, leaves were collected and measured before fall (green) and during fall (orange / yellow) A standard branch reflectance of 8.6% was applied to all tree branches.

Shown in Figure 3, each tree portrays a gradient of colours. White represents when there are no leaves on the tree. The bar transitions from the white gradient into its summer colour when the leaves start growing in the spring. The summer colour then transitions into the fall colour. Finally, when the leaf drop occurs, the fall colour than translates back into white. The precise colorimetric measurements are included on GitHub.

Tree Model Generation

Figure 4: Malus floribunda tree branch and crown model.

Twelve tree canopy models of full leaf foliage and realistic branch systems were created. Moderate polygon (3,000-10,000 triangles) tree trunk and branch models were generated using an author-modified version of proctree.js (Brunt & Green, 2017) based on depictions of leafless trees in *The Architecture of Trees* (Leonardi & Stahi, 2019). Generation parameters such as branch lengths, maximum and minimum clumping, gravity, radius, climb rate, trunk length, and total number of branches were matched to the depictions.

Full-leafed canopies (< 20,000 triangles) were generated following the algorithm published by Balakrishnan and Jakubiec (2020) surrounding these tree branch models and falling within the previously discussed measured tree height and canopy diameter parameters. Leaf clustering search distance parameters were selected to match the visible appearance of actual tree canopies. Generated canopy-only gap percentages following Balakrishnan and Jakubiec (2020), which did not consider branches within canopies, were increased based on total branch length, diameter, and

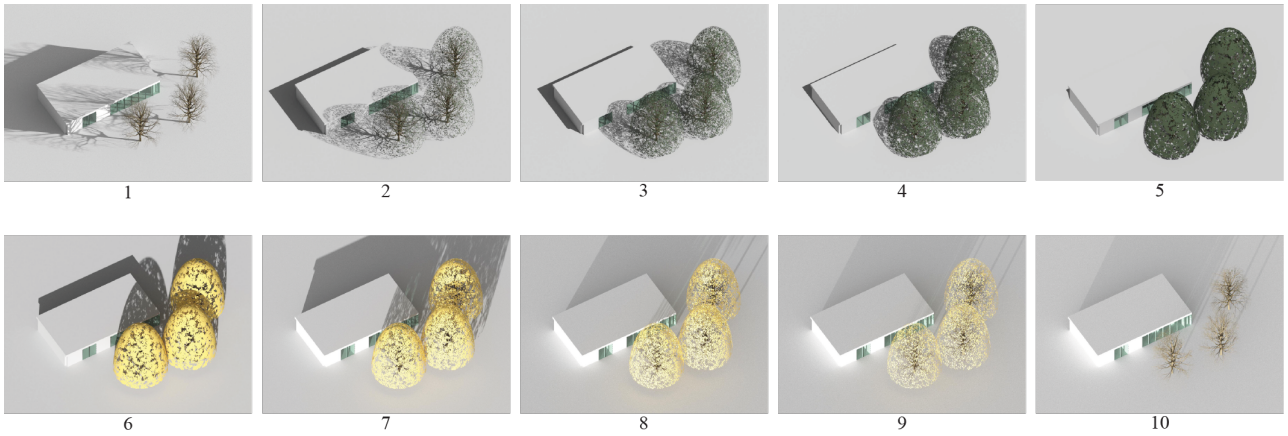

(1) Bare Branches. Feb 14 - Mar 27
(2) 25% Leaf Growth. Mar 27 - Apr 10
(3) 50% Leaf Growth. Apr 10 – 21
(4) 75% Leaf Growth. Apr 21 - July 14
(5)100% Leaf Growth. July 14 - Oct 15
(6) Leaf Colour Change, Oct 15 - Nov 11
(7) 25% Leaf Drop. Nov 11 - 22
(8) 50% Leaf Drop. Nov 22 - Dec 4
(9) 75% Leaf Drop. Dec 4 -15
(10) 100% Leaf Drop. Dec 15 - Feb 14

Figure 5: Betula pendula's leaf senescence stages in simulations.

an estimated overlap projection to match the photographically measured data. The branch and canopy generation parameters are included on GitHub with an example model shown in Figure 4. Measured reflectance properties were applied to each generated canopy and trunk in the Radiance material format (Ward, 1994).

Simulation Processes

Daylight modelling

An open office simulation model was used with south and east-facing glazing and no urban contextual obstructions. Material properties of this space are assigned as per the IES LM-83 (2012) suggestions for opaque materials. A glazing with 61% visible light transmittance was applied to glazing surfaces, and a roller blind with 2.2% direct normal permeability and 5.4% diffuse transmission was modelled as a dynamic roller blind material adjacent to each glazing surface. A sensor grid with a spacing of 0.6 m between sensors and at an elevation of 0.8 m above the finished floor was applied uniformly throughout the space. Figure 6 displays the geometry of this model as well as the daylight sensor grid.

For simulating the effect on daylight that each of the twelve trees have within the space, three-dimensional tree models with geometric and material properties as defined in the previous section are located at the centroids of three squares depicted in red in Figure 6. Deciduous tree models are categorized into five leaf fullness states (1. bare branches, 2. 25% leaf presence, 3. 50% leaf presence, 4. 75% leaf presence, 5. 100% leaf presence) and two colour states (1. summer, 2. autumnal) which results in nine different unique states for each tree according to our temporal implementation (see Figure 5).

A brute force approach is applied such that annual daylight and glare simulations are run for all hours for each of the nine states. A hybrid climate-based daylight modelling approach is used where direct sunlight is calculated at each

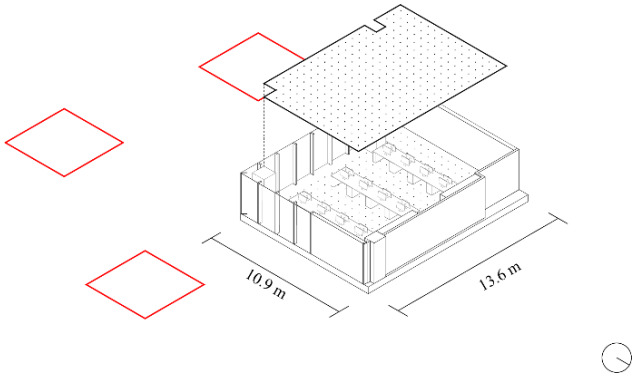

Figure 6: Open office simulation model, exploded sensor grid, and tree placement.

hour using precise solar positions, and illuminance is calculated using the Radiance 3-phase method (*ClimateStudio*, 2021; McNeil & Lee, 2012) and Perez sky models (Perez et al., 2020) based upon climate data for Vancouver, BC, Canada. For each simulation model, roller blind state was considered for each window group (south, east) following IES LM-83 (2012) such that no more than 2% of the floor area was illuminated by direct sunlight exceeding 1000 lx. Tree-specific annual schedules of leaf presence and colour change (see Figure 3*)* were used to select indoor illuminance levels and window shading states at each hour to produce an annual climate-based daylighting result influenced by deciduous trees with dynamic foliage and coloration. Dimming of electric lights was modelled based on the mean spatial daylight levels at each occupied hour such that the electric lighting fraction is defined as in Equation 1 for a target illuminance of 500 lx, where EL_{frac} is the fractional power use of electric lighting and $\overline{E_h}$ is the mean grid sensor illuminance in lux. The minimum fractional lighting level is 0.

$$EL_{frac} = 1.0 - \overline{E_h}/500$$

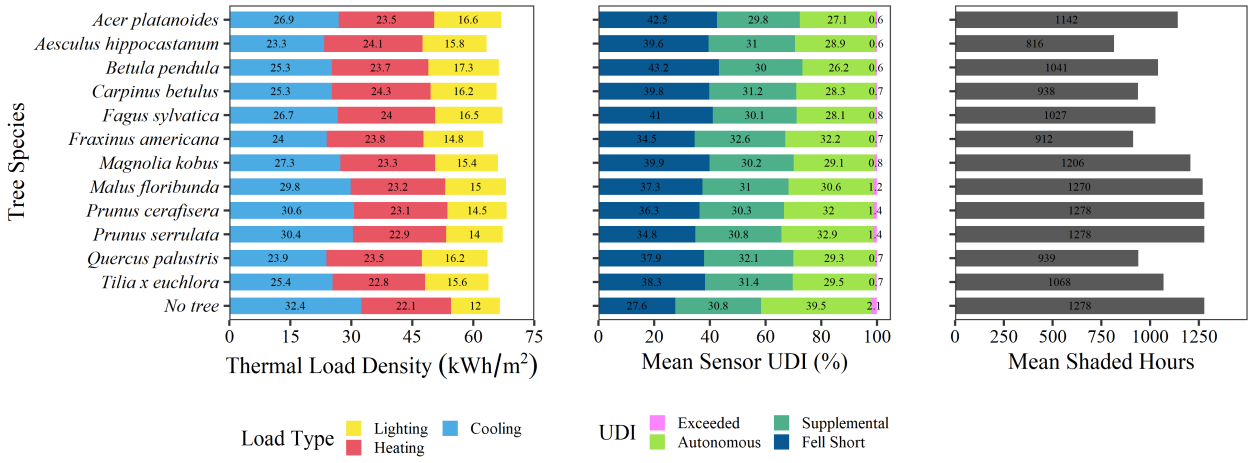

Figure 7: Simulation results of the Thermal Load Density, Mean Sensor UDI, and Mean Shaded Hours.

Thermal modelling

An equivalent thermal model is produced based on a typical office building. Windows (Tvis 61%, SHGC 37%, U 1.66 W/m^2-K) are modelled using the same properties as the daylight model. Exposed walls have a U-value of 0.178 W/m^2-K, and the ground slab has a U-value of 0.48 W/m^2-K. Other walls and the zone ceiling are modelled as adiabatic adjacencies. Occupant density, lighting power density, and equipment power density are 18.5 m^2/person, 10.8 W/m^2, and 10.8 W/m^2 respectively. Operational schedules follow that of a typical medium office building. Window shades (7% transmission) operate following the daylight schedules for the south and east glazing calculated based on IES LM-83 (2012) from the daylight model. Air leakage is constant at 0.1 ACH while 12.5 L/s/p is provided by a mechanical ventilation system with a 70% efficient heating recovery ventilator. The thermal models were built and simulated using EnergyPlus version 9.4.0 (Crawley et al., 2001).

Our tree models (up to 30,000 triangles per tree) would slow EnergyPlus's shading calculations to the point of uselessness, therefore, daylit fractions are calculated using raytracing based on hourly direct and diffuse radiation simulations. A grid of sensors spaced on a 10 cm grid are created at each window grid and simulated with and without the presence of trees in each of the nine tree phenology states. Based on the ratio of shaded-to-unshaded irradiation for each state, a 10-minute (interpolated) sunlit fraction schedule is provided to EnergyPlus for each window, thus avoiding the need for geometric shading calculations during the thermal simulation process (Luo et al., 2021).

Results

Simulation Results with Different Tree Species

Each of the twelve species (and no trees) were simulated with dynamic foliage, colour change, and dynamic blinds, and the outcomes are shown in Figure 7. Three groups of data are presented: thermal load densities, mean sensor UDI values, and the mean number of hours where roller blinds are closed. The thermal load density shows annual thermal loads of the office space showing the differences in heating, cooling, and lighting demand. The mean sensor UDI shows the difference in daylight level distribution between four categories of illuminance ranges (Fell Short <100lx, Supplemental 100-300lx, Autonomous 300-3000lx, Exceeded >3000lx). The mean shaded hours graph shows the average amount of time that the south and east roller blinds are closed.

The mean annual thermal load density for all species is 65.8 kWh/m^2, where the 'No tree' simulation has a load density of 66.5 kWh/m^2 and the best performing model (*F. americana*) has a load density of 62.5 kWh/m^2, 5% less than the mean and 6% less than no tree at all. Daylight levels, calculated with dynamic shades also differ meaningfully across simulation results. UDI$_s$ summed with UDI$_a$ is a good descriptor of beneficial daylight access (ranging from 100 lx – 3000 lx) throughout the year. The 'No tree' simulation has the highest mean UDI$_{s+a}$ of 70.3%, while the *F. americana* performed the second best with a UDI$_{s+a}$ of 64.8% and the worst performer (*B. pendula*) has a UDI$_{s+a}$ of 56.2%. These daylighting levels should be assessed relative to the amount of time window shades are closed for each model. The 'No tree' model along with two smaller tree models (*P. cerafisera* and *P. serrulata*) have the longest occupied time with blinds closed, 1,278 h. The *F. americana* model has blinds closed only 913 h, a 28.7% reduction. A. hippocastanum planted around the windows yields the lowest amount of 815 h of blinds closed, a 36.1% reduction.

Tree Model Simplification and Effect on Results

We ran the annual daylight and energy simulation five times: with dynamic foliage and leaf colour change (presented in the previous subsection), with dynamic foliage and no leaf colour change, with evergreen trees, with an opaque tree with no change (as recommended by LM-83), and with no tree at all. Figure 8 is a boxplot of variance distributions comparing the four simplified simulations to the detailed tree model with measured transmittance, dynamic foliage, and dynamic colour. Variance for each result is calculated by the below equation,

$$Variance_{simple-tree} = \frac{100 \cdot R_{full-tree}}{R_{simple-tree} - R_{full-tree}}$$

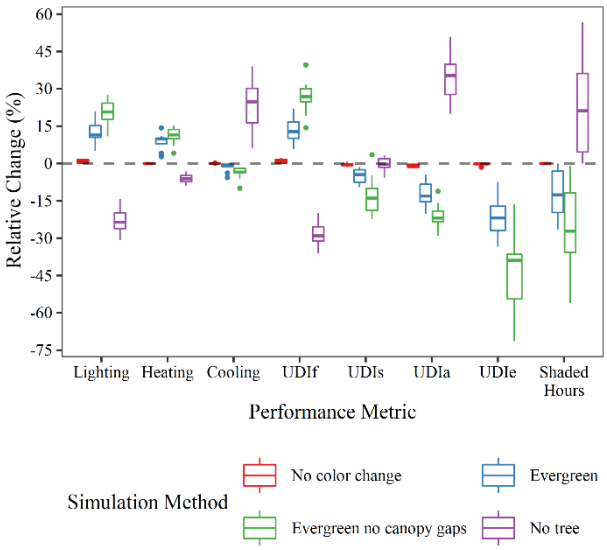

Figure 8: Variance of other simulation techniques compared to the best practice.

Positive change values indicate that the simplified model causes an increase in a result proportional to its result while negative change values indicate the opposite.

Colour change has almost no effect on energy use, useful daylight illuminance, or shade utilization. Evergreen tree models with canopy caps, not accounting for seasonal leaf phenology, increase predicted lighting energy use by 12.3%

and increase heating loads by 8.8% while underpredicting shade use by 12.4% on average. These evergreen models decrease mean UDIs and mean UDIa by 5.0% and 12.6% respectively compared to the detailed baseline. Evergreen trees without canopy gaps (as recommended per IES LM-83) increase these discrepancies: lighting energy use increased by 20.7% and heating loads increase by 11.2% while model shade use drops by 25.6%. Such opaque, evergreen tree canopies decrease autonomous daylight (UDIa) by 21.1% on average. Finally, simulations with no trees at all reverse such trends. Models without trees lead to a 23.0% underprediction in lighting energy use, a 6.1% reduction in heating loads, and a 23.1% increase in cooling loads on average. Autonomous daylight (UDIa) is 34.5% higher on average.

In Figure 8, the UDIe for 'No tree' models is excluded from the figure as it exceeds other relative changes by a significant margin (median relative change = 189.1%; mean = 167.4%).

Discussion

The interaction between dynamic landscape elements and building performance is not typically considered in sustainable architectural design nor building performance simulations. We illustrate the impact of having detailed trees in simulations through the development of a new model of deciduous trees in integrated annual daylight and electric lighting calculations. We benchmarked the impact of such considerations by comparing them to modelling methods more common in practice such as using evergreen tree models, opaque tree canopies (such as in IES LM-83), or not accounting for trees at all. Beyond a new calculation method, this paper illustrates that interactions between landscape, shading operation, visual comfort, lighting, and energy can have significant impacts for daylit spaces near the ground or for planted facades.

Simulation of the Dynamic Landscape

One important thing to consider is, what does it mean for designers to be able to simulate dynamic landscape elements? On a practical level, designers would have access to new decision-making tools about decorative tree selection and more accurate models. For example, out of the twelve deciduous trees, *Fraxinus americana* is the best performing species for this planting arrangement and climate (Vancouver). The results in Figure 7 show that it contributes to the lowest thermal load density of all species. In addition, useful daylight illuminance levels for the *Fraxinus americana* are optimal when compared to other tree species. On average its UDIs and UDIa have higher values (32.6% and 32.2% respectively) compared to *Betula pendula* (30% and 26.2%), for example. The tree also contributes to a low number of mean shaded hours (912 hours) compared to *Betula pendula* (1041 hours) and no tree (1278 hours), providing more hours for exterior views to be accessed.

Predicted Effects on Building Operation

As illustrated by Figure 8, results in spaces shaded by landscape can vary substantially by how deciduous trees are represented in simulations. Following an IES LM-83 modelling procedure with opaque evergreen trees, UDIa can vary by as much as 28.9% (*Q. palustris*) and shade use by as much as 56.1% (also *Q. palustris*) compared to our detailed dynamic models of the same tree. In the case of simulating with no tree at all, these results can be even more extreme. We conclude that better representation of dynamic landscape elements in spaces where they significantly interact with incoming daylight could have significant impacts on results presented to decision makers and therefore resulting design considerations.

Simulation Time

A limitation of the methodology used to create the detailed tree models presented in this paper are that it is time and data intensive. In the case of simulation time, the tree and branch models are geometrically complex, composed of up to 30,000 triangles per tree. In addition, we consider up to 9 tree states considering leaf colour and senescence. Using the detailed tree models and our 'brute force' approach for dynamic leaf colour and senescence, simulations took approximately 60 times longer than a simple LM-83 opaque model using a spherical, evergreen representation of a tree.

A Pilot Database of Trees

Much of the source data for our models (Figures 3 and 4) are not easily found in literature. To accurately portray the dynamic features of trees, numerous types of data are required: gap fraction, canopy dimensions, colour information, and temporal schedules of leaf drop and leaf regrowth. Tree and leaf phenology data is not often collected, where dates of leaf drop, and regrowth periods may vary depending on climate, geographical location, and whether the tree is in an urban or forest environment. Gap fraction data is not commonly seen in literature, where the Balakrishnan & Jakubiec (2020) method is used to measure the gap fractions for the models used in this paper.

In response to this, a library of our twelve common Vancouver deciduous trees containing tree models and data will be accessible to the public. In addition, the measurement code and tree-generation code will be shared via GitHub: https://github.com/C38C/tree_database.

Communication to Designers

Figure 9 compares the annual daylight and shade use an office space with no trees, *F. americana*, and *B. pendula*. The figure illustrates the temporal distribution of blind closure for each window group that is influenced by the surrounding trees and its effect on annual daylight distributions. The top of the figure shows three floor plans comparing the sum percent of occupied hours of UDIs and

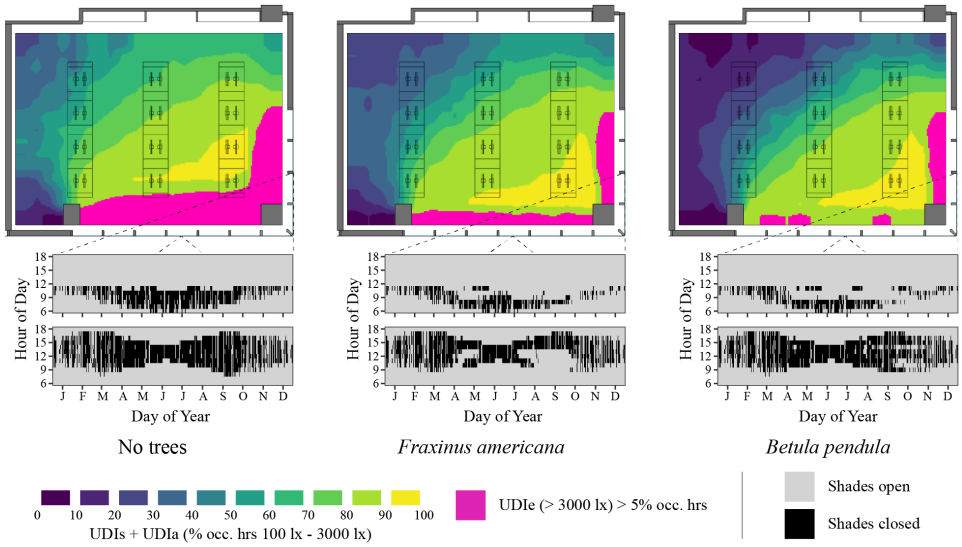

Figure 9: Daylight and shade use comparisons of an office space with no trees, F. americana, and B. pendula.

UDIa which accounts for illuminance values between 100 lx – 3000 lx. Pink spaces on the plan depict UDIe (> 3000 lx) occurring more than 5% of occupied hours (Reinhart & Wienold, 2011). The diagrams below the plans show the hours of shades open and closed for the south and east windows. This figure illustrates the reduction in shade closure for east-facing and south-facing windows during April to October.

Future Work and Implementation

Given the expensive computational cost of the method proposed in this paper, future work, including implementation in accessible daylight simulation tools, should address this. Enhancements to Radiance multi-phase raytracing methods, for example, could be extended to account for dynamic exterior elements. The method might also be streamlined by using the 5-phase method directly, only recomputing the daylight matrix seasonally. Such approaches would also be useful in accounting for other seasonal changes such as snowfall, something daylight simulation has largely ignored.

Much user effort and simulation time could also be saved by using low-polygon tree models. While these have limitations for glare analysis, for our model using reduced 100 polygon trees resulted in a 57 s energy simulation time (with pixel counting), removing the need to run EnergyPlus with pre-calculated shaded fractions. 500 polygon trees took 298 s, and 1000 polygon trees took 714 s. Daylight simulations would have reduced speed improvements.

Conclusion

This paper describes a new scheme of creating detailed, dynamic deciduous tree models which will lead to increased accuracies in building simulations. The current paradigm of tree models has been simple geometries with an applied transmittance coefficient, however, often neglecting tree phenology patterns. Our tree models are seasonally varying through the integration of tree canopy gap fractions. This was done by scheduling leaf drop, regrowth, and colour change dates according to each species in the climate of Vancouver, British Columbia, Canada, or nearby geographical areas. The typical dimensions, heights, and colours of tree canopies are also included for each species. The twelve most common deciduous street trees in Vancouver were studied and measured from June to July 2021 during their full leaf foliage. Our research proves that dynamic trees and tree species selection can impact daylight and energy simulation results due to differing canopy dimensions, gap fractions, and leaf drop and regrowth schedules.

Acknowledgement

The authors acknowledge funding support for Jessie Pan from the NSERC Undergraduate Student Research Grant.

References

Akbari, H., Pomerantz, M., & Taha, H. (2001). Cool surfaces and shade trees to reduce energy use and improve air quality in urban areas. *Solar Energy*, *70*(3), 295–310.

Balakrishnan, P., & Jakubiec, J. A. (2016). *Measuring Light Through Trees for Daylight Simulations: A Photographic And Photometric Method*.

Breen, P. (n.d.). *Oregon State University, Department of Horticulture | Landscape Plants*. Retrieved September 28, 2021, from https://landscapeplants.oregonstate.edu/

Brunt, P., & Green, B. (2017). *Proctree.js* [JavaScript]. https://github.com/supereggbert/proctree.js/

ClimateStudio. (2021). https://www.solemma.com/climatestudio

Coder, K. (2017, January). *Identified Benefits of Community Trees & Forests*. https://www.warnell.uga.edu/outreach/publication

s/individual/identified-benefits-community-trees-forests

Compagnon, R. (2004). Solar and daylight availability in the urban fabric. *Energy and Buildings*, *36*(4), 321–328.

Crawley, D. B., Lawrie, L. K., Winkelmann, F. C., Buhl, W. F., Huang, Y. J., Pedersen, C. O., Strand, R. K., Liesen, R. J., Fisher, D. E., Witte, M. J., & Glazer, J. (2001). EnergyPlus: Creating a new-generation building energy simulation program. *Energy and Buildings*, *33*(4), 319–331.

De Jaegere, T. (2016). *A Review of the Characteristics of Small-Leaved Lime (Tilia cordata Mill.) and Their Implications for Silviculture in a Changing Climate*.

Donovan, G. H., & Butry, D. T. (2009). The value of shade: Estimating the effect of urban trees on summertime electricity use. *Energy and Buildings*, *41*(6), 662–668.

Fu, Y. H., Piao, S., Delpierre, N., Hao, F., Hänninen, H., Liu, Y., Sun, W., Janssens, I. A., & Campioli, M. (2018). Larger temperature response of autumn leaf senescence than spring leaf-out phenology. *Global Change Biology*, *24*(5), 2159–2168.

Gilman, E. F., & Watson, D. G. (1993). *680 Tree Fact Sheets*. Institute of Food and Agricultural Sciences, University of Florida. https://hort.ifas.ufl.edu/database/trees/trees_scientific.shtml

Hwang, W. H., Wiseman, P. E., & Thomas, V. A. (2016). *Simulation of Shade Tree Effects on Residential Energy Consumption in Four U.S. Cities*. 23.

Leonardi, C., & Stahi, F. (2019). *The Architecture of Trees*. Princeton Architectural Press.

Luo, X., Tang, Y., & Hong, T. (2021). *Efficient Computation Of Surface Sunlit Fractions In Urban-Scale Building Modeling Using Ray-Tracing Techniques*. Lawrence Berkeley National Lab. (LBNL), Berkeley, CA (United States).

McNeil, A., & Lee, E. (2012). A validation of the Radiance three-phase simulation method for modelling annual daylight performance of optically complex fenestration systems. *Journal of Building Performance Simulation*, *6*, 1–14.

McPherson, G. E., Nowak, D. J., & Rowntree, R. A. (1994). *Chicago's urban forest ecosystem: Results of the Chicago Urban Forest Climate Project* (NE-GTR-186; p. NE-GTR-186). U.S. Department of Agriculture, Forest Service, Northeastern Forest Experimental Station.

Moesker, K. (2019). *Magnolia Kobus: a Study of the Popular Horticultural Species and its Recent Invasion of Native Ecosystems in Ontario, Canada*. *58*, 21.

Nasrollahi, N., & Shokri, E. (2016). Daylight illuminance in urban environments for visual comfort and energy performance. *Renewable and Sustainable Energy Reviews*, *66*, 861–874.

Nobis, M., & Hunziker, U. (2005). Automatic thresholding for hemispherical canopy-photographs based on edge detection. *Agricultural and Forest Meteorology*, *128*(3), 243–250.

Observational Data | USA National Phenology Network. (2021). https://www.usanpn.org/data/observational

Observations. (2021). INaturalist. https://www.inaturalist.org/observations

Pausas, J. G. (1997). Litter fall and litter decomposition in Pinus sylvestris forests of the eastern Pyrenees. *Journal of Vegetation Science*, *8*(5), 643–650.

Perez, R., Michalsky, J., & Seals, R. (2020). *Perez Sky Model*.

Reinhart, C.F., Wienold, J. (2011). The daylighting dashboard - A simulation-based design analysis for daylit spaces. *Building and Environment, 46*(2), 386-396.

Schaber, J., & Badeck, F.-W. (2005). Plant phenology in Germany over the 20th century. *Regional Environmental Change*, *5*(1), 37–46. https://doi.org/10.1007/s10113-004-0094-7

Simpson, J. R. (2002). Improved estimates of tree-shade effects on residential energy use. *Energy and Buildings*, 10.

Simpson, J. R., & McPherson, E. G. (1998). Simulation of tree shade impacts on residential energy use for space conditioning in Sacramento. *Atmospheric Environment*, *32*(1), 69–74.

Simpson, J. R., & McPherson, E. G. (2003). Potential energy savings in buildings by an urban tree planting programme in California. *Urban Forestry & Urban Greening*, *2*(2), 73–86.

Szkordilisz, F., & Kiss, M. (2016). Passive cooling potential of alley trees and their impact on indoor comfort. *Pollack Periodica*, *11*(1), 101–112.

The Daylight Metrics Committee. (2012). *IES LM-83-12* (1st ed.). Illuminating Engineering Society.

Ticknor, R. L. (1973). *Landscape Tree Performance*. Oregon State University.

Tregenza, P., & Wilson, M. (2011). *Daylighting: Architecture and Lighting Design.* Routledge.

Villalba, A., Pattini, A., & Correa, E. (2014). An approach to urban tree daylight permeability simulation using models based on louvers. *Building and Environment*, *73*, 75–87.

Ward, G. J. (1994). The Radience lighting simulation and rendering system. *Proceedings of the 21st Annual Conference on Computer Graphics and Interactive Techniques - Siggraph '94*, 459–472.

Wilkinson, D. M. (1995). Modelling Tree Crowns as Geometric Solids. *Arboricultural Journal*, *19*(4), 387–393.